

## Proton spin-lattice relaxation in TMMC $[(\text{CH}_3)_4\text{NMnCl}_3]^\dagger$

Daniel Hone and Claudio Scherer\*

*Physics Department, University of California, Santa Barbara, California 93106*

Ferdinando Borsa<sup>†</sup>

*Istituto di Fisica dell'Universita, 2700 Pavia, Italy*

(Received 17 August 1973)

We examine the temperature and frequency dependence of the proton spin-lattice relaxation rate  $1/T_1$ , as a probe of the electron-spin dynamics of the quasi-one-dimensional exchange-coupled paramagnet TMMC  $[(\text{CH}_3)_4\text{NMnCl}_3]$ . The rate is measured from 5.5–16 MHz and from 1.4 °K to room temperature. An extension of Moriya's magnetic-relaxation theory to the linear-chain system, using the exact classical results for static spin-correlation functions, gives over-all good quantitative agreement between theory and experiment. A sharp minimum in  $1/T_1$  at  $T \simeq 18$  °K, an  $\omega^{-1/2}$  dependence on frequency at room temperature and  $\omega^{-3/2}$  at low temperature, with the external field parallel to the chain, and the frequency independence of  $1/T_1$  at room temperature with the field perpendicular to the chain are all explained by the theory.

### I. INTRODUCTION

The special features of spin dynamics in one dimension, notably the long-time persistence of spin correlations, have been shown<sup>1</sup> to have dramatic consequences for the behavior of exchange-narrowed EPR linewidths and line shapes. However, the dipolar-broadened EPR line is described in terms of a four-spin dynamic correlation function whose calculation has proved feasible only within a decoupling, or independent-mode approximation. The long-wavelength diffusive behavior of the resulting two-spin correlation functions, or dynamic wave-vector-dependent susceptibilities, dominates the theoretical prediction for the EPR lines. On the other hand, nuclear spin-lattice relaxation rates are given directly by these two-spin functions, so that a study of the field and temperature dependence of these rates gives direct access to the low-frequency spectral weight of the spin fluctuations. A direct comparison with theory is possible without the necessity for any decoupling approximation.

Of the numerous magnetic linear-chain crystals which have been investigated, the one exhibiting the most nearly ideal one-dimensional behavior appears to be  $(\text{CH}_3)_4\text{NMnCl}_3$ , or TMMC. We have measured the proton spin-lattice relaxation time  $T_1$  in this material from 1.4 °K to room temperature, at resonant frequencies ranging from 5.5 to 16 MHz at low temperatures, and up to 80 MHz at 300 °K. More extended measurements of the frequency dependence of  $T_1$  at room temperature will be presented together with measurements in  $\text{CsMnCl}_3 \cdot 2\text{H}_2\text{O}$  in a separate publication.<sup>2</sup> The low-temperature behavior of  $T_1$  has been measured independently<sup>3</sup> at 25 MHz and discussed briefly on the basis of a spin-wave picture. It is difficult to systematically include in this way the effects of

spin-wave damping or of the contributions of diffusive modes to the low-frequency spectral weight, and extension to substantially higher temperatures of this theory is not feasible. The self-consistent theory of Blume and Hubbard<sup>4</sup> for calculating dynamic spin-correlation functions in three-dimensional Heisenberg systems has recently been extended<sup>5</sup> to linear Heisenberg chains by carefully incorporating the effects of short-range order which are so important in these materials. The agreement found with neutron-scattering data was excellent. However, we have chosen to use a simpler theoretical approach, based on the techniques originally employed<sup>6</sup> by Moriya to study  $T_1$  in three-dimensional exchange-coupled paramagnets, in order to maintain analytical expressions for  $T_1$  to as late a stage in the calculation as possible and to give as clear a physical picture as we can of the origin of the contributions to the relaxation rate. We make maximal use of the static spin-correlation functions of the classical Heisenberg linear chain, known<sup>7</sup> for all temperatures. The necessary parameters for TMMC are well known, with the exception of some uncertainty in the relevant proton positions at low temperatures, and we find good quantitative agreement with the frequency and temperature dependence of  $T_1$  over most of the experimental range investigated.

The experimental procedures are discussed in Sec. II, and the theoretical model is presented in Sec. III. The numerical predictions of the theory and comparison with experiment are given in Sec. IV.

### II. EXPERIMENT

A large single crystal of TMMC was grown by slow evaporation from a dilute (~10%) HCl solution of almost equimolar  $\text{MnCl}_2 \cdot 4\text{H}_2\text{O}$  and

$(\text{CH}_3)_4\text{NCl}$  salts. The crystal was cut and mounted on a sample holder so that the  $c$  axis could be rotated in a plane containing the magnetic field direction.

The proton spin-lattice relaxation rate was measured at 5.5, 8, and 16 MHz using a pulsed phase-coherent cross-coil magnetic-resonance spectrometer.<sup>8</sup>

For temperatures above about 40 °K the free-precession decay,  $S(t)$ , is nearly Gaussian with a dephasing time  $\tau$ , defined as  $S(\tau) = S(0)e^{-1}$ , which is slightly temperature dependent. Furthermore, since the sample was not ellipsoidal, the free-precession decay was linearly field dependent due to the inhomogeneous broadening coming from the nonuniform demagnetizing factor. At 300 °K the extrapolation to zero external magnetic field yields  $\tau \approx 70 \mu\text{sec}$ , for  $\hat{c} \perp \vec{H}_0$ , and it agrees with the field-independent value measured in a spherical sample.

At temperatures lower than 40 °K, the free-precession decay narrows and displays a structure which depends on the orientation of the magnetic field with respect to the crystalline axis. This is in agreement with a previous study by continuous-wave techniques of the proton resonance in TMMC.<sup>9</sup> In fact, in the latter work it was found that the shape of the proton absorption line is dominated by the nuclear dipole-dipole interaction. Above 40 °K the  $\text{CH}_3$  group undergoes hindered rotations which partially average out the dipolar interaction. However, the Gaussian shape observed at room temperature is an indication that the averaging is not complete and that the line shape is still dominated by secular terms in the nuclear dipolar interaction, with a negligible nonsecular contribution coming from the dipolar interaction of the protons with the  $\text{Mn}^{2+}$  magnetic ions.

The spin-lattice relaxation rate was measured by a 90°-90° or 180°-90° pulse sequence. The decay was found to be exponential over almost two decades. The recovery of the nuclear magnetization, i. e.,  $\ln | [M(t) - M_0] / 2M_0 |$  versus  $t$ , yields a slope which does not depend on the exact length of the first pulse. For  $T < 40$  °K the resonance spectrum is split into four lines, but the measurements of  $T_1$  were found to be independent of the exact value of the external magnetic field at fixed frequency.

In order to vary the temperature we used a double-wall cryostat with the sample directly immersed in a refrigerant fluid. For the temperature range 1.4–4.2 °K liquid helium was used; for  $10.2 \leq T \leq 20.4$  °K hydrogen; for 24.8–27.2 °K neon; for  $55 < T < 90$  °K oxygen. Additional measurements from 4.2 to 50 °K were performed while the cryostat was slowly warming up after all the liquid coolant had evaporated, and the temperature was continuously monitored with a gold (0.02-at. %-iron)-chromel thermocouple. Since these mea-

surements had to be done very quickly, we used the null-point method, where the relaxation rate is simply determined from the time  $t_0$  at which the magnetization is zero after the first 180° rf pulse. Because the line is not completely saturated,  $M(t=0)$  is not in fact precisely  $(-M_0)$ . Then the measured  $t_0$  must be corrected (by about 20%) to give the true recovery time from saturation, and thereby  $T_1$ . Consequently, the estimated experimental error in both  $T_1$  and  $T$  is larger for these measurements than for the others (approximately  $\pm 10\%$ , rather than  $\pm 5\%$ ). The measurements in the range 90–300 °K were performed by Mali in Pavia with a standard nitrogen-gas-flow system.

### III. THEORETICAL MODEL

The very definition of a spin-lattice relaxation time  $T_1$  presumes an exponential decay law for the longitudinal magnetization,

$$C(t) \equiv \frac{\langle I^z(t) I^z(0) \rangle}{\langle (I^z)^2 \rangle} \approx e^{-t/T_1}, \quad (3.1)$$

for all times  $t$  of importance ( $t \sim T_1$ ). By standard techniques, employing a formal perturbation expansion of  $I^z(t)$  and a cumulant expansion of the resulting expression for  $C(t)$ , keeping only the lowest-order nonvanishing term,<sup>10</sup> we have the approximate relation

$$\ln C(t) \propto \int_0^t d\tau (t - \tau) \langle [I^z(\tau), \mathcal{H}'(\tau)] \times [\mathcal{H}', I^z] \rangle, \quad (3.2)$$

which agrees with Eq. (3.1) for times longer than the characteristic decay time of the correlation function in the integrand. Here  $\mathcal{H}'$  is the hyperfine Hamiltonian (of dipolar origin in the present case):

$$\mathcal{H}' = \sum I_n F_{nj} S_j \quad (3.3)$$

and all operators are given in the interaction representation. Then the correlation functions of interest are of the form  $\langle S_q(\tau) S_{-q}(0) \rangle$ , with  $q$  a wave vector in the first Brillouin zone. Their decay rate is set by the exchange interaction strength  $J$ , and is therefore in general very rapid on the time scale  $T_1$  of interest, except that at long wavelengths (small  $q$ ) the rate also vanishes with  $q^2$ . That is, on general hydrodynamic grounds the long-wavelength dynamics of a Heisenberg chain are governed by a diffusion equation. In three dimensions the phase-space volume factor diminishes the importance of these small- $q$  values, and the exponential form (3.1) is approximately correct (this just corresponds to the standard exchange-narrowing theory), but the relative importance of small- $q$  values in one dimension is precisely what leads to the long-time persistence of spin correlations in linear chains, and the resultant unusual properties of EPR lines there.<sup>1</sup> How-

ever, the nuclear time scale,  $t \sim T_1$ , is so long that the dipolar interactions, both within a single chain and between spins on different chains, has become effective in damping the spin correlations.<sup>11</sup> We will therefore include an exponential factor  $e^{-\Gamma_d t}$ , with  $\Gamma_d$  of the order of the electronic dipolar coupling strength, in the spin-correlation functions wherever necessary and thereby recover an exponential decay for  $C(t)$  for times  $t$  of interest in the nuclear spin relaxation.

In terms of the hyperfine tensor  $F$  defined by Eq. (3.3) and the above assumption on sufficiently rapid decay of the spin-correlation functions, we have<sup>6</sup> for the nuclei at equivalent positions  $r_p$

$$\frac{1}{T_1} = \frac{1}{2\hbar^2} \int_{-\infty}^{\infty} dt \cos(\omega_n t) \sum (F_{pj}^{\nu\nu'} + iF_{pj}^{\nu\nu'}) \times (F_{pj'}^{\nu\nu'} - iF_{pj'}^{\nu\nu'}) \langle \{S_j^\nu(t) S_{j'}^{\nu'}(0)\} \rangle, \quad (3.4)$$

where the sum is over  $j, j', \nu$ , and  $\nu'$ ;  $\nu, \nu' = x, y, z$ ; the nuclear Zeeman frequency is  $\omega_n$ ; and  $\{AB\}$  denotes the symmetrized product  $\frac{1}{2}(AB + BA)$ . In TMMC the three-dimensional magnetic ordering temperature  $T_n \approx 0.8^\circ\text{K}$  implies an exchange coupling between chains of at most the order of the dipolar coupling, so we will ignore correlations between spins on different chains. For the particular case of an external field  $H_0$  parallel to the chains, or  $c$  axis, Eq. (3.4) becomes

$$\frac{1}{T_1} = \frac{(\hbar\gamma_e\gamma_n)^2}{4\pi} \int dt \cos(\omega_n t) \int dg \left( \frac{1}{4} A_p^+(q) \langle \{S_q^+(t) S_{-q}^-(0)\} \rangle + A_p^z(q) \langle \{S_q^z(t) S_{-q}^z(0)\} \rangle \right), \quad (3.5)$$

where the coefficients  $A(q)$  are the Fourier transforms of the spherical components of the product of two dipole-interaction tensors:

$$A_{pjj'}^+ = \frac{(1 - 3\cos^2\theta_{pj})(1 - 3\cos^2\theta_{pj'}) + 9\sin^2\theta_{pj}\sin^2\theta_{pj'}}{r_{pj}^3 r_{pj'}^3}, \quad (3.6)$$

$$A_{pjj'}^z = \frac{9\sin\theta_{pj}\cos\theta_{pj}\sin\theta_{pj'}\cos\theta_{pj'}}{r_{pj}^3 r_{pj'}^3},$$

$$A_p^\alpha(q) = \sum A_{pjj'}^\alpha e^{i\mathbf{q}\cdot(\mathbf{r}_j - \mathbf{r}_{j'})}. \quad (3.7)$$

Here the polar angles  $\theta_{pj}$  are defined relative to the  $c$  axis and  $j'$  and  $j$  are restricted to be on the same chain (because the correlation functions vanish otherwise), so that  $q$  is a scalar wave vector,  $-\pi \leq q \leq \pi$  in units of the inverse separation between neighboring magnetic ions along a chain.

Now it is convenient to write the correlation functions in terms of the corresponding relaxation functions,

$$R_q^\alpha(t) = (S_q^\alpha(t), S_q^{\alpha\dagger}(0)) \equiv \int_0^\beta d\lambda \langle S_q^\alpha(t - i\hbar\lambda) S_q^{\alpha\dagger}(0) \rangle, \quad (3.8)$$

where  $\beta = 1/k_B T$ ,  $\alpha = +, -, \text{ or } z$ , and the static susceptibility is given by

$$\chi^\alpha(q) = (g\mu_B)^2 R_q^\alpha(0). \quad (3.9)$$

The connection between correlation and relaxation functions is

$$\int_{-\infty}^{\infty} dt e^{i\omega t} \langle S_q^\alpha(t) S_q^{\alpha\dagger}(0) \rangle = \frac{1}{2} \hbar \omega \coth\left[\frac{1}{2}(\beta\hbar\omega)\right] R_q^\alpha(\omega), \quad (3.10)$$

where  $R(\omega)$  is the Fourier transform of  $R(t)$ . It will be convenient to extract explicitly from the time dependence of the spin operators that part due to the Zeeman Hamiltonian, so that the remaining dynamics will be governed solely by exchange. Then the relevant values of  $\omega$  in Eq. (3.10) will be  $\omega_n$  or  $\omega_e$ , the nuclear or electronic Zeeman frequency, and, except at the lowest temperatures and highest fields with  $\omega = \omega_e$ ,

$$\frac{1}{2} \hbar \omega \coth\left[\frac{1}{2}(\beta\hbar\omega)\right] \approx 1/\beta. \quad (3.11)$$

Having replaced the spin-correlation functions in the expression (3.5) for  $1/T_1$  by the corresponding relaxation functions, we write the latter in the convenient form

$$R_q^\alpha(t) = (g\mu_B)^{-2} \chi^\alpha(q) f_q^\alpha(t), \quad (3.12)$$

which effectively extracts the thermodynamic static response function  $\chi^\alpha(q)$  from the normalized relaxation function  $f_q^\alpha(t) = R_q^\alpha(t)/R_q^\alpha(0)$ . The susceptibility  $\chi^\alpha(q)$  is known at all temperatures for the linear Heisenberg chain, at least in the classical spin limit.<sup>7</sup> Measurement of  $\chi(q=0)$  in TMMC shows<sup>12</sup> excellent agreement with the classical spin theory, indicating that  $S = \frac{5}{2}$  (for  $\text{Mn}^{2+}$ ) is large enough to be treated classically for determining the static properties even at temperatures of a few degrees kelvin. The uniform susceptibility is quite anisotropic below about  $20^\circ\text{K}$ , and it was necessary to include the effects of magnetic dipole interactions between Mn spins to obtain agreement with experiment. However, at low temperatures we will find we need  $\chi(q \approx \pi)$ . At  $q=0$  the maximum anisotropy is less than a factor of 2. It may well be more important in the critical  $q = \pi$  fluctuations, but in the absence of any better theory we take for simplicity the isotropic form of  $\chi(q)$  which, at least, exhibits the important thermodynamic instability  $\chi(\pi) \rightarrow \infty$  as  $T \rightarrow 0$ :

$$\chi^\alpha(q) = \frac{1}{2} \chi^*(q) = \frac{C/T}{a + b \cos q}, \quad (3.13a)$$

$$a = (b^2 + 1)^{1/2} = \frac{1 + u^2}{1 - u^2}, \quad (3.13b)$$

$$u = \frac{1}{K} - \coth K, \quad K = 2\beta JS(S+1) \quad (3.13c)$$

where  $J$  has been defined to be positive for the antiferromagnetic coupling in TMMC. We mention

parenthetically that the form (3.13a) for  $\chi$  is also the result of molecular-field theory (but with  $a=1$ ;  $b=\Theta/T$ ), and that with the inclusion of the Onsager reaction field (equivalent to the spherical model)<sup>13</sup> we also recover Eq. (3.13b), but  $u$  must be redefined. We have used the latter results in a treatment of resonance behavior in three-dimensional exchange-coupled paramagnets.<sup>14</sup>

There remains then the problem of the determination of the normalized relaxation functions  $f_q^\alpha(t)$ . We follow Mori and Kawasaki<sup>15</sup> (and Moriya<sup>6</sup>) by writing  $f_q^\alpha(t)$  in terms of relaxation of the torques, or time derivatives of the spin operators, which in general are not subject to the hydrodynamic conservation laws appropriate to  $S_q^\alpha$  as  $q \rightarrow 0$ , and therefore decay more rapidly in time. Then we write

$$f_q^\alpha(t) = 1 - \int_0^t (t-\tau) |\dot{f}_q^\alpha(\tau)| d\tau \approx e^{-\Gamma_q^\alpha t}, \quad (3.14)$$

$$\Gamma_q^\alpha = \int_0^\infty d\tau |\ddot{f}_q^\alpha(\tau)|$$

for  $t \gg \tau_q$ , where  $\tau_q$  is the characteristic decay time of  $\dot{f}_q^\alpha(t)$ . If we further make the standard Gaussian assumption

$$\ddot{f}_q^\alpha(t) \approx \ddot{f}_q^\alpha(0) e^{-t^2/\tau_q^2}, \quad (3.15)$$

and if  $\Gamma_q \tau_q \ll 1$  so that the exponential decay (3.14) is already appropriate for  $t < \Gamma_q^{-1}$ , then  $\tau_q$  and  $\Gamma_q^\alpha$  can be determined by the second and fourth frequency moments of  $f_q^\alpha$ :

$$\begin{aligned} M_n^\alpha(q) &= \int \frac{d\omega}{2\pi} \omega^n f_q^\alpha(\omega) \\ &= i^n \frac{d^n}{dt^n} f_q^\alpha(t) \Big|_{t=0}, \end{aligned} \quad (3.16)$$

$$\tau_q^2 = 2M_2/M_4, \quad \Gamma_q^\alpha = (\pi M_2^2/2M_4)^{1/2}. \quad (3.17)$$

The moments are given explicitly<sup>16</sup> as

$$M_2 = \frac{-8Ju(1 - \cos q)(a + b \cos q)}{\beta}, \quad (3.18)$$

$$\begin{aligned} M_4/M_2 &= 8J^2S(S+1)[(1+u/K)(1-u-3\cos q+2u \\ &\quad \times \cos^2 q + 3/u) + 1 + (1-2u)\cos q - 2/u], \end{aligned}$$

where the quantities  $u$  and  $K$  are defined by Eq. (3.13c). We will later find that at high temperatures ( $K \ll 1$ ) the important contributions arise from  $q \ll 1$  (the lowest-energy fluctuations  $\sim q=0$ ) and at low temperatures ( $K \gg 1$ ) they are from  $Q \equiv (\pi - q) \ll 1$  (critical fluctuations, large susceptibility near  $q = \pi$ ). In these limits

$$M_2 \approx \frac{1}{3} [8J^2S(S+1)q^2], \quad (3.19a)$$

$$M_4/M_2 \approx \frac{1}{3} [16J^2S(S+1)], \quad K, q \ll 1$$

$$M_2 \approx 16J^2S(S+1)(Q^2 + K^{-2}),$$

$$M_4/M_2 \approx 16J^2S(S+1)(Q^2 + K^{-1}), \quad (3.19b)$$

$$K^{-1}, Q = (\pi - q) \ll 1.$$

We point out that  $M_4$  does not satisfy the scaling requirement that it be a function only of  $QK$  (the correlation length  $\xi = K$ ), although  $M_2$  does. However, in the critical region  $Q \lesssim K$ , we can neglect the  $Q$  dependence of  $M_4/M_2$  in Eq. (3.19b) altogether. Since both  $M_2$  and  $M_4$  are proportional to  $q^2$  for small  $q$  (and all  $\beta$ ), this yields the long-wavelength diffusive behavior of  $f_q^\alpha(t)$  with the usual diffusion coefficient,  $\Gamma_q \approx Dq^2$ . In fact, the above procedure is equivalent to the assumption<sup>17</sup>

$$f_q^\alpha(\omega) = 2\Gamma_q^\alpha e^{-\omega^2 \tau_q^2} [\omega^2 + (\Gamma_q^\alpha)^2]^{-1}. \quad (3.20)$$

This single-central-mode structure for  $f_q(\omega)$ , or, equivalently, for the dynamic structure factor  $S(q, \omega)$ , leaves out the important short-range correlations which result in well-defined short-wavelength spin waves at low temperatures and a corresponding three-peak form for  $f_q(\omega)$ . However, we are interested in the low-frequency behavior to determine  $T_1$ . Insofar as the long-wavelength contribution dominates, the theory should be valid, and it may not be seriously in error for contributions from  $q$  close to  $\pi$  where the spectral weight is again concentrated at small  $\omega$ .<sup>16</sup> In fact, once short-range order at  $q = \pi$  becomes established, the dynamical fluctuations near  $q = \pi$  are of long wavelength for the local *magnetic* lattice of twice the crystal lattice spacing. Although this form cannot properly account for the contributions from the spectral tails of higher-energy spin waves, we would not expect this to be important either at high temperatures or at temperatures sufficiently low that the spin-wave peaks are relatively sharp. Furthermore, the theory has the advantage of analytical and physical simplicity.

We turn next to the question of the modifications due to the dipolar coupling between electrons. This will introduce a further source of decay<sup>11</sup> of  $f_q^\alpha(t)$ , which we can represent for simplicity by an additional factor  $e^{-\Gamma_d t}$  in those functions, with  $\Gamma_d$  of the order of the dipolar interaction energy. The effect is to replace  $\Gamma_q^\alpha$  in Eq. (3.20) by  $\Gamma_q^\alpha + \Gamma_d$ , which is important only at small  $q$  because exchange is so much stronger than the dipole interactions. Thus we need not be concerned with any  $q$  dependence of  $\Gamma_d$ . Further, the inclusion of  $\Gamma_d$  is inessential in (3.20) if  $\omega \gg \Gamma_d$ , which is the case for  $\omega = \omega_e$  in the external magnetic fields considered here. We then require the dipolar decay only for the longitudinal fluctuation contribution to  $1/T_1$ , or  $\alpha = z$ , where  $\omega = \omega_n$ . Finally, then, we have

$$\frac{1}{T_1} = \frac{1}{T_1^*} + \frac{1}{T_1^{\#}} \quad , \quad (3.21a)$$

$$\frac{1}{T_1^*} = (\hbar\gamma_e\gamma_n)^2 \frac{S(S+1)}{12} \beta \hbar \omega_e \coth\left(\frac{\beta \hbar \omega_e}{2}\right) \\ \times \int_{-\pi}^{\pi} \frac{dq}{2\pi} \left( \frac{A_p^*(q)}{a + b \cos q} \right) \left( \frac{\Gamma_q^*}{\omega_e^2 + (\Gamma_q^*)^2} \right) \quad , \quad (3.21b)$$

$$\frac{1}{T_1^{\#}} = (\hbar\gamma_e\gamma_n)^2 \frac{S(S+1)}{6} \int_{-\pi}^{\pi} \frac{dq}{2\pi} \\ \times \left( \frac{A_p^*(q)}{a + b \cos q} \right) \left( \frac{1}{\Gamma_q^* + \Gamma_d} \right) \quad , \quad (3.21c)$$

where the geometrical factors  $A(q)$  are given by Eqs. (3.6) and (3.7), the coefficients  $a$  and  $b$  in the susceptibility by Eq. (3.13), and the relaxation rates  $\Gamma_q^*$  by Eq. (3.17). We have taken  $\omega_n = 0$ , since it is negligible with respect to both  $\omega_e$  and  $\Gamma_d$ . For most values of temperature and field which we will consider,  $\coth[\frac{1}{2}(\beta \hbar \omega_e)] \approx [\frac{1}{2}(\beta \hbar \omega_e)]^{-1}$ , but we retain the more general form in (3.21b).

Before considering explicit numerical results we comment on some of the general features of the expression (3.21) for  $1/T_1$ . The frequency, or external-field, dependence is all contained in the transverse contribution  $1/T_1^*$ . At high temperatures ( $K \ll 1$ ) we have from (3.13) that  $u \approx -\frac{1}{3}K \propto \beta$ ,  $a = 1 + O(\beta^2)$ ,  $b = O(\beta)$ , and  $\chi(q) = C/T$ . The dominant contribution to the integral in (3.21b) comes, as one would expect, from small  $q$ , and the frequency dependence is determined by

$$\frac{1}{T_1^*} \propto \int_0^{\infty} \frac{dq}{\pi} A_p^*(0) \frac{Dq^2}{\omega_e^2 + (Dq^2)^2} \propto (D\omega_e)^{-1/2} \quad , \\ \frac{1}{T_1} \approx A\omega_e^{-1/2} + B \quad \text{for } K \ll 1 \quad , \quad (3.22)$$

as expected from one-dimensional diffusion-dominated spin dynamics.

At low temperatures  $K \gg 1$ ,  $u \approx 1/K - 1$ ,  $a \approx K \propto \beta$ ,  $b = a - O(1/\beta)$ , and  $\chi(q) \sim \beta(a + b \cos q)^{-1}$  becomes large near  $q = \pi$ , reflecting the tendency toward antiferromagnetic ordering. There is a corresponding slowing down in  $\Gamma_q$  near  $q = \pi$ ; from Eq. (3.19b) we see that, for low temperatures ( $K \gg 1$ ) and for  $Q^2 \ll K^{-1} \ll 1$ , where  $Q = \pi - q$ ,

$$\Gamma_q \approx D'(Q^2 + K^{-2})K^{1/2} \quad , \quad (3.23)$$

where  $D' = 8\pi^2 S(S+1)$  and  $K$  appears as a correlation length. In fact, the static susceptibility in the same region ( $Q$ ,  $K^{-1} \ll 1$ ) has similar behavior,

$$\chi(q) \approx C/(Q^2 + K^{-2}) \quad , \quad (3.24)$$

which explicitly exhibits the role of  $K$  as a correlation length. Then the dominant contribution to  $T_1^*$ , from the region  $Q \lesssim K^{-1}$  is given by

$$\frac{1}{T_1^*} \sim \int_0^{\infty} dq \frac{TK^2\Gamma(Q=0)}{\omega_e^2 + \Gamma^2(Q=0)(Q^2 + K^{-2})^2 K^4} \quad . \quad (3.25)$$

For  $\omega_e \ll \Gamma(Q=0) = D'/K^{3/2}$  (above a few degrees kelvin for TMMC with  $\nu_n \sim 10$  MHz)  $\omega_e$  can be neglected, and  $1/T_1^*$  (and indeed  $1/T_1$ ) is predicted<sup>18</sup> to decrease as  $T^{-3/2}$ . At lower temperatures we can neglect  $K^{-2}$  in Eq. (3.25) (although not in  $1/T_1^{\#}$ ) and we expect

$$1/T_1 \approx A'\omega^{-3/2} + B' \quad , \quad K \gg 1 \quad , \quad \omega_e K^{3/2}/D' > 1 \quad . \quad (3.26)$$

As we have noted above, the approximations of the theory are most questionable in this low-temperature region. We cannot expect to have correctly treated the immediate vicinity of the three-dimensional ordering temperature ( $T_N \sim 0.84$  °K for TMMC), but we find (see Fig. 9) that there does appear to be a small range of temperatures in TMMC where Eq. (3.26) is valid.

Finally, we point out that  $T_1$  will exhibit a peak as a function of temperature. Both the inverse of the diffusion constant  $D^{-1}$  and  $T\chi(0)$  behave like  $(1 - A^2\beta)$  for small  $\beta$ , so that both  $1/T_1^*$  and  $1/T_1^{\#}$  decrease as the temperature is reduced from large values. The low-temperature behavior depends somewhat on the parameters of the system, but, as discussed above, there is a region in which  $1/T_1$  is approximately<sup>18</sup> proportional to  $\beta^{3/2}$ . There is therefore a minimum of  $1/T_1$  at some intermediate temperature ( $\sim 18$  °K in TMMC). The low-temperature behavior was discussed by Richards<sup>3</sup> on the basis of the very different undamped-spin-wave model, involving direct magnon emission processes, which predicts  $1/T_1 \propto \beta$  in its simplest form. The steeper rate of decrease found in the present theory is more in accord with the experimental behavior of  $1/T_1$  (see, however, Ref. 18). At sufficiently low temperatures  $1/T_1^*$  exhibits a maximum and may lead to a flattening of  $1/T_1$  below that temperature.

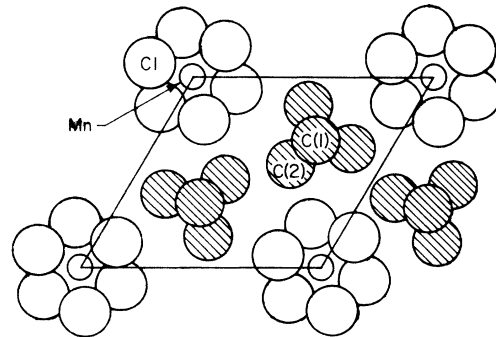


FIG. 1. Structure of TMMC as viewed along magnetic chains. Carbons of  $(\text{CH}_3)_4\text{N}$  groups shaded.

#### IV. NUMERICAL RESULTS: COMPARISON WITH EXPERIMENT

In the spirit of treating TMMC as a classical Heisenberg linear chain, at least as far as its static magnetic properties are concerned, we have chosen a value of the exchange constant  $J \approx 7^\circ \text{K}$ , consistent with a fit<sup>12</sup> of the uniform-susceptibility data to the classical theory. What is of principal importance is that we have used a temperature-independent value of  $J$ , which then just sets the temperature scale. The susceptibility, from (3.13), depends on  $J$  only as  $\beta J$ , and from Eqs. (3.17) and (3.18) we see that the same is true for  $\Gamma_q/J$ . Therefore, our results for  $J/T_1$  for fixed frequency  $\omega/J$  (and  $\Gamma_d/J$ ) will be independent of  $J$  except for an over-all temperature-scaling factor. Superexchange interactions are highly sensitive to geometry. Although there is a structural phase transformation at about  $128^\circ \text{K}$  in TMMC, with unknown influence on the Cl-ion positions, and the Mn nearest-neighbor separation increases gradually with decreasing temperature (approximately a 1% increase from 300 to  $4^\circ \text{K}$ )<sup>19</sup>, the low-temperature value of  $J$  deduced from the spin-wave spectrum observed in inelastic neutron scattering<sup>19</sup> is in close agreement with the higher-temperature susceptibility value.<sup>12</sup>

The proton positions, required for calculation of the dipolar sums  $A(q)$ , are much less well known, as discussed in Sec. II. In view of the considerable present uncertainty in the position of the protons we have chosen a model which places them on the average at the carbon positions deduced from the high-temperature x-ray data.<sup>20</sup> The few-percent changes in interchain separations associated with the structural transformation have little effect on the dipole sums, but any substantial re-orientation of the TMA groups or freezing out of

rotations would. We will consider below the modification in  $1/T_1$  associated with changes in the proton positions, but first we take them at the carbon positions labeled 1 and 2 in Fig. 1. (For the external field  $\vec{H}_0$  parallel to the chains, there are three equivalent "2" positions in each tetramethylammonium group.) Finally, we point out that the interaction between protons is sufficiently strong ( $T_2 \ll T_1$ ) that energy exchange takes place readily between inequivalent protons, and the single measured  $1/T_1$  represents a weighted-average transfer rate to the lattice of the various protons.

We consider quantitatively only the case with  $\vec{H}_0$  parallel to the  $c$  axis. From Eqs. (3.6) and (3.7) we see that only three separate dipole sums are required, namely,

$$\sum \frac{e^{iqz}}{r_{pj}^3}, \quad \sum \frac{\cos^2 \theta_{pj} e^{iqz}}{r_{pj}^3},$$

and

$$\sum \frac{\sin \theta_{pj} \cos \theta_{pj} e^{iqz}}{r_{pj}^3},$$

where  $z_j$  is the coordinate of the  $j$ th Mn spin along its chain axis. The contributions fall off rather slowly with distance along a chain, but we found rapid convergence by the time ten spins on either side of the closest Mn spin were included for each of the six closest chains to a given proton. The results for  $A_p^+(q)$  and  $A_p^z(q)$  for protons at the two carbon sites  $C(1)$  and  $C(2)$  are given in Fig. 2. The general behavior can be understood from symmetry considerations, as shown in Fig. 3. Let us choose the origin of the  $z$  axis (parallel to the chains) at a Mn position and take length units of the nearest-neighbor Mn separation ( $\equiv \frac{1}{2}c$ , where  $c$  is the unit cell dimension along the chain so that  $z_j = j$ ). If the proton labeled  $p$  has a  $z$  coordinate of 0 or 0.5,

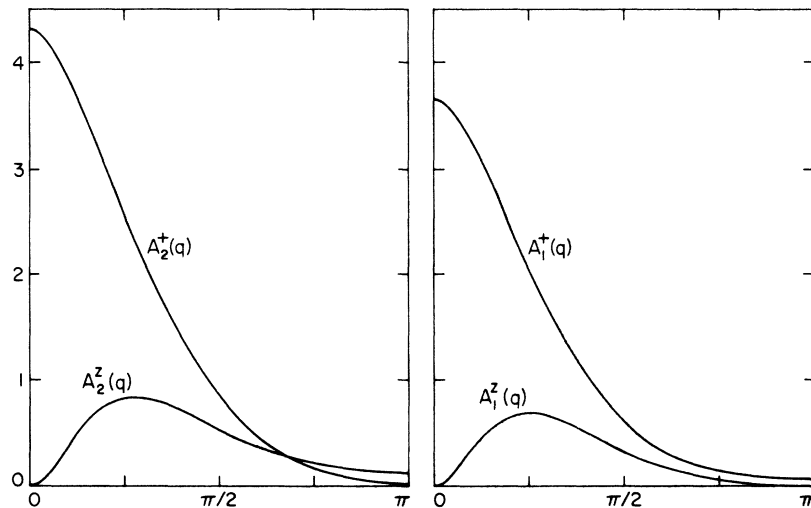


FIG. 2. Geometrical (dipolar) sums  $A_i^+(q)$  [Eqs. (3.6) and (3.7)] for nuclei at the carbon positions  $C(i)$  ( $i=1$  or  $2$ ).

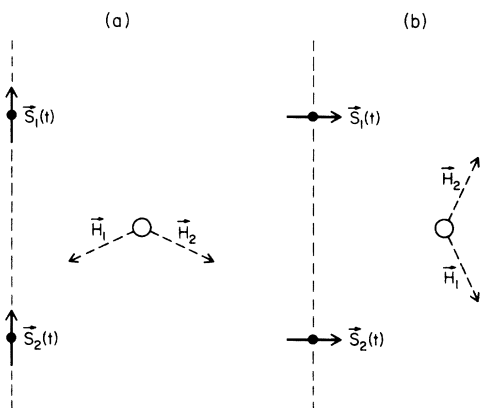


FIG. 3.  $\vec{S}_1(t)$  and  $\vec{S}_2(t)$  are representative (not necessarily near-neighbor) spins giving dipolar fields  $\vec{H}_1$  and  $\vec{H}_2$  at the site of the proton, indicated by a circle.  $\vec{H}_0 \parallel \hat{c}$ . (a) Transverse field at nucleus located on mirror plane at  $z=0$  (plane contains an electron spin) or  $z=0.5$  (plane is bisector of line connecting near-neighbor spins) vanishes for longitudinal fluctuation at  $q=0$ . Similarly, it vanishes for  $q=\pi$  if  $z=0$ , and is maximal at  $q=\pi$  if  $z=0.5$  (reverse one of fields shown). (b) Transverse field is maximal at nucleus for  $q=0$  if  $z=0$  or  $0.5$ , or for  $q=\pi$  and  $z=0$ , and vanishes for  $q=\pi$  and  $z=0.5$ .

then  $\sin\theta_{pj} \cos\theta_{pj}/r_{pj}^3$  is an odd function of  $j$  and  $A_p^\pm(q=0)=0$ . In fact, because of the relatively long range of the interaction,  $A_p^\pm(q=0)$  is sufficiently small for *any* proton position that the small- $q$  contribution ( $\Gamma_q < \Gamma_d$ ) to  $1/T_1^*$  [see Eq. (3.21c)] is negligible for any reasonable value of  $\Gamma_d$ . Our results are then insensitive to the cutoff associated with

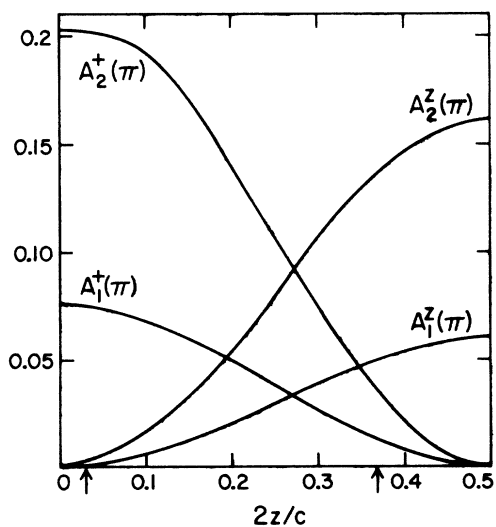


FIG. 4. Geometrical (dipolar) factors  $A_i^\pm(q=\pi)$  for nuclei located at the horizontal positions C(1) and C(2) of Fig. 1, as functions of the vertical position  $z$ .

$\Gamma_d$ . The transverse fields at the nucleus which contribute to  $T_1$  processes tend to cancel for a  $q=0$  longitudinal spin fluctuation, as can be seen readily from the geometry (Fig. 3). Similarly for  $q=\pi$ , where the phase factors alternate in sign,  $e^{i\pi j} = (-1)^j$ , it is easily seen that  $A^\pm(\pi)=0$  for a proton at  $z=0$  and  $A^+(\pi)=0$  for a proton at  $z=0.5$ . In Fig. 4 we show the sensitivity of  $A^\pm(\pi)$  to the proton  $z$  coordinate for the two horizontal positions corresponding to C(1) and C(2). In contrast we find, as suggested above, that  $A^\pm(0)$  is virtually unaffected by changes in the proton  $z$  coordinate. The long-wavelength behavior is also relatively insensitive to the  $xy$  coordinates of the proton, particularly after summation over all neighboring chains of spins, so the high-temperature results (dominated by small  $q$ ) depend very little on the choice of proton coordinates in the model.

In Fig. 5 the predictions of the theory, with no adjustable parameters, are compared with the proton  $1/T_1$  data at room temperature, for  $\vec{H}_0$  parallel to the  $c$  axis, as a function of frequency  $\nu_n$ . The theory is for a proton at the position of C(2). The results for a proton at C(1) are only about 10% smaller, and, as discussed above, the observed relaxation rate should be a weighted average for the inequivalent protons. The various approximations of the theory are expected to be most accurate at high temperatures, and the agreement with experiment, including the  $\omega_e^{-1/2}$  dependence of diffusion-dominated dynamics predicted by Eq. (3.22), is excellent. The contrasting lack of frequency dependence of  $1/T_1$  for  $\vec{H}_0 \perp c$ , also shown in Fig. 5, just means  $1/T_1^* \gg 1/T_1$  for this case, and it can

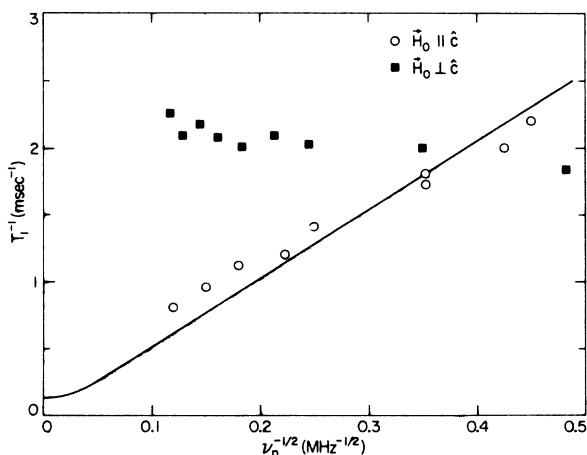


FIG. 5. Nuclear relaxation rate  $1/T_1$  as a function of frequency. The circles are experimental points and the curve the theoretical prediction for  $\vec{H}_0 \parallel \hat{c}$  with no adjustable parameters. The choice of  $\nu_n^{-1/2}$  as abscissa clearly exhibits the frequency dependence (3.22). The experimental values for  $\vec{H}_0 \perp \hat{c}$  are indicated by squares.

again be understood on the basis of Fig. 3. At high temperatures we recall that the major contribution to  $1/T_1$  is from long-wavelength fluctuations  $q \approx 0$ . The contribution  $1/T_1^z$  was small with  $\vec{H}_0 \parallel \hat{c}$  because of the geometrical cancellation of the transverse components of the dipolar fields associated with the longitudinal fluctuations, as indicated in Fig. 3(a). Such cancellation does not occur for  $\vec{H}_0 \perp \hat{c}$ , if the vector from the nucleus to the chain axis is neither parallel nor perpendicular to  $\vec{H}_0$ . But the azimuthal angles  $\varphi_p$  of the protons (relative to a chain as polar axis) are distributed over a broad range of values, and the longitudinal fluctuations at  $q=0$  will give substantial transverse fields at most of them. Moreover, for small  $q$  we have  $f_q^+(\omega_e) \sim Dq^2/\omega_e^2$ , whereas  $f_q^z(0) \sim 1/\Gamma_d$ . Therefore, if the geometrical factors are comparable, as we have suggested, the spectral weight  $f_q^z(\omega)$  at the nuclear resonance frequency  $\omega \approx 0$  associated with the longitudinal fluctuation can be so much larger than  $f_q^+(\omega_e)$  that  $1/T_1^z$ , which is intrinsically independent of frequency, will dominate the behavior of  $1/T_1$ .

The experimental proton relaxation rates at nuclear resonance frequencies  $\nu_n = 5.5, 8,$  and  $16$  MHz, and for  $\vec{H}_0 \parallel \hat{c}$ , are plotted as functions of temperature in Fig. 6. The corresponding theoretical curves, again for a proton at the C(2) position, are given in Fig. 7. We reemphasize that there has been no adjustment of parameters in these results. In addition to the agreement at room temperature we find the minimum in  $1/T_1$  of approximately the observed size and at very nearly the observed temperature (which is almost independent of frequency). The principal failures of the theory include an insufficiently sharp dip and the lack of substantial frequency dependence at low temperatures. The low-temperature theoretical

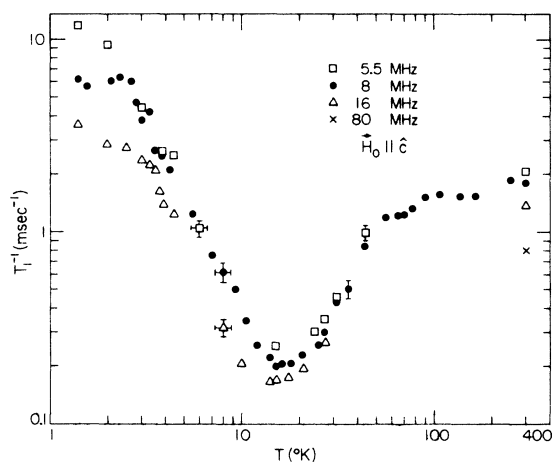


FIG. 6. Experimental nuclear relaxation rates  $1/T_1$  vs temperature for  $\nu_n = 5.5, 8, 16,$  and  $80$  MHz, for  $\vec{H}_0 \parallel \hat{c}$ .

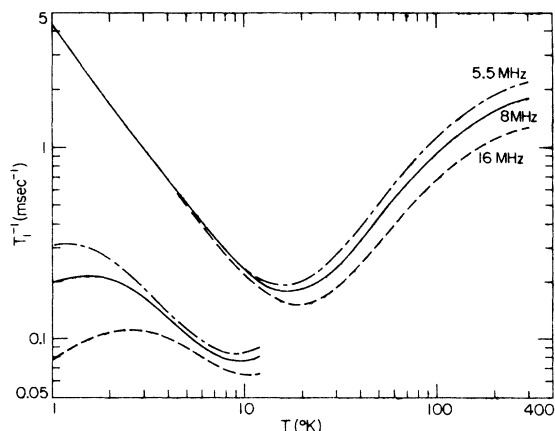


FIG. 7. Theoretical prediction corresponding to the experimental curves of Fig. 6. The curves in the lower left-hand corner represent the contributions of transverse fluctuations  $1/T_1^z$  alone for low temperatures.

frequency-dependent contributions, from the transverse spin fluctuations, are also shown in the figure. They exhibit qualitatively the observed behavior, but their numerical contribution to  $1/T_1$  is too small. These features can be seen more clearly in Fig. 8, where a direct comparison of theory and experiment is made for a nuclear-resonance frequency of  $8$  MHz.

One might anticipate a jump in  $1/T_1$  at the structural phase transition near  $128^\circ\text{K}$  associated with an abrupt change in proton positions, but none was observed experimentally. There may be a gradual change in position (or motion), which might explain

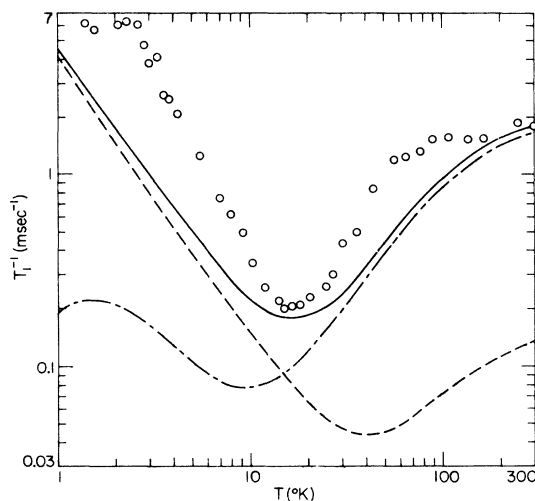


FIG. 8. Detailed comparison of theory (no adjustable parameters) and experiment for  $1/T_1$  at  $8$  MHz. The solid line is the theoretical  $1/T_1$ , the dashed curve  $1/T_1^z$ , and the dot-dashed curve  $1/T_1^+$ .



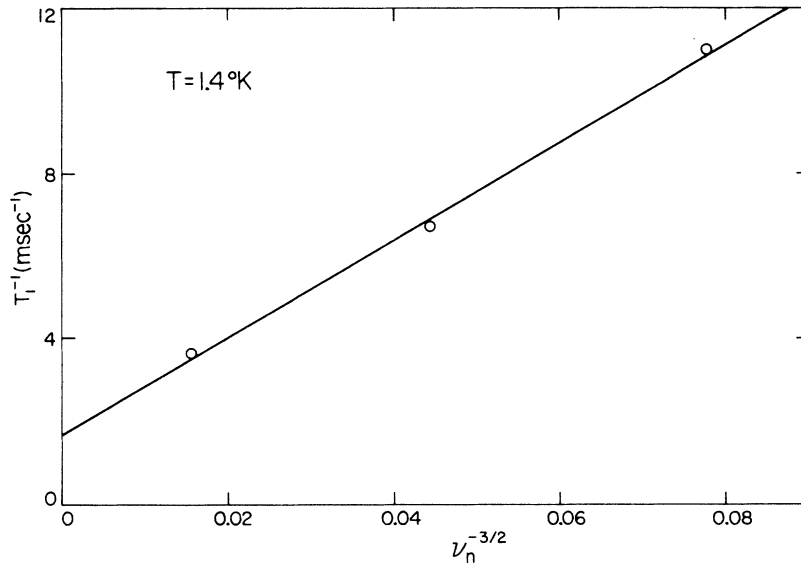


FIG. 9. Frequency dependence of  $1/T_1$  at  $1.4^\circ\text{K}$ , showing the  $\nu_n^{-3/2}$  dependence predicted by Eq. (3.26). The curve here is a straight line fitted to the experimental points—not the numerical result of the theory, as in Fig. 5.

the unexpectedly weak temperature dependence of  $1/T_1$  above  $60^\circ\text{K}$ . The proton-resonance line shape does change character at that temperature.<sup>9</sup> The position of the minimum in  $1/T_1$  might not be changed much; we found it to be relatively insensitive to the proton position. This point may be clarified with data on the  $^{15}\text{N}$  nuclear relaxation in TMMC, and these experiments are presently being planned.

The behavior at low temperatures can also be fitted by a suitable (temperature-dependent) choice of proton position. For  $4 < T < 12^\circ\text{K}$ ,  $T_1$  is found to be nearly frequency independent, as predicted [see Eq. (3.25) and the discussion following it], although the temperature dependence is more nearly  $T^{-2}$  than the  $T^{-3/2}$  predicted.<sup>18</sup> Furthermore, the observed frequency dependence of  $1/T_1$  at the lowest temperature,  $1.4^\circ\text{K}$ , can be successfully fitted to the form given in Eq. (3.26), as shown in Fig. 9. However, in spite of this apparent success of the present theory, we know that the approximations tend to break down at low temperatures, and we must consider to what extent the behavior determining  $T_1$  might be altered. First, the classical spin theory, used both for  $\chi(q)$  and for the moments which determine  $\Gamma_q$ , may no longer be accurate for describing the spin- $\frac{5}{2}$  system. However, the classical theory does appear to work well for the uniform susceptibility,<sup>12</sup> if the effects of dipolar anisotropy are included. The anisotropy may be important in  $\chi(q=\pi)$  as well, but its influence on the dynamics in  $f_q^\alpha(\omega)$  is a more likely source of trouble. We know that once fluctuation energies are comparable to anisotropy energies there can be a “crossover” to critical behavior characteristic of the lower symmetry.<sup>21</sup> For an

easy magnetic axis this would give Ising-like critical behavior; for the actual case of  $xy$  anisotropy the form of the critical behavior (for  $S = \frac{5}{2}$ ) is not known. Because the anisotropy is set by the intrachain rather than interchain dipole strengths, this crossover should occur well above that to three-dimensional critical behavior.<sup>22</sup> Finally, there is the assumption of a cutoff Lorentzian form (3.20) for  $f_q(\omega)$ . For  $q$  sufficiently close to  $\pi$ ,  $Q = \pi - q \ll 1$ , there is some indication that  $f_q(\omega)$  may still have a single-peak structure.<sup>16</sup> Spin waves will be well defined only for  $Q = \pi - q \gtrsim \xi^{-1}$ , where  $\xi (=K)$  is the static correlation length. If this single peak is to have our assumed cutoff Lorentzian shape, then the formalism of Sec. III [see Eqs. (3.14) and (3.15) and the related discussion] re-

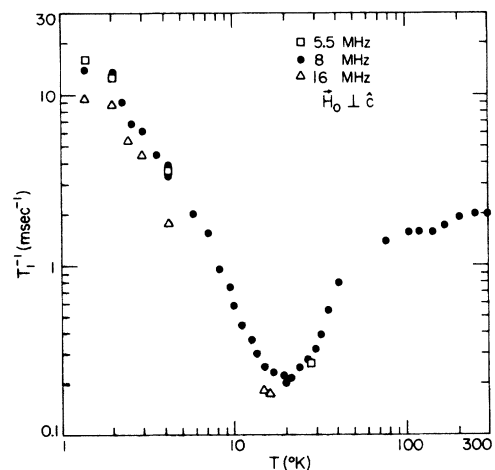


FIG. 10. Experimental relaxation rates  $1/T_1$  vs temperature for  $\nu_n = 5.5, 8,$  and  $16\text{ MHz}$ , with  $\vec{H}_0 \perp \hat{c}$ .

quires  $\Gamma_q \tau_q \ll 1$ . From Eq. (3.19b) we have for low temperatures ( $K \gg 1$ ) and for  $Q \ll 1$

$$\Gamma_q \tau_q = \frac{\sqrt{\pi} M_2^2}{M_4} \approx (\sqrt{\pi}) \frac{Q^2 + K^{-2}}{Q^2 + K^{-1}} \quad (Q, K^{-1} \ll 1), \quad (4.1)$$

which is indeed small compared to unity for  $Q \lesssim K^{-1}$ , the important values of  $Q$  contributing to  $1/T_1^*$  at temperatures of interest. In that case we are looking at the spectral weights  $f_q(\omega)$  at  $\omega = 0$ . However, for the transverse-spin-fluctuation contribution  $1/T_1^*$  we need the spectral weight at  $\omega_e$ , and if spin waves are well defined at energies of the order of  $\omega_e$  then there is substantially more spectral weight at the frequency than implied by the Lorentzian approximation. We take the spin-wave energy  $E(Q) = 4JS \sin Q$  to be well defined for  $Q > \xi^{-1}$ , where  $\xi \approx K$  at low temperatures. Then we have

$$E(Q = \xi^{-1}) \approx 4JS/K = 0.6T \quad (4.2)$$

for TMMC. For  $\nu_n \sim 10$  MHz we have  $\omega_e \sim 0.3^\circ\text{K}$ , suggesting important spin-wave effects at the lowest experimental temperatures. We are investigating the predictions of a more sophisticated theory to compare with the low-temperature experiments.

Finally, we give in Fig. 10 the results of proton relaxation rates  $1/T_1$  measured with the field perpendicular to the  $c$  axis. We see qualitatively

the same temperature dependence, but much less frequency dependence, as discussed above. The geometrical relations are much more complex for this case, and, considering the uncertainties in the proton positions, we have not attempted a numerical calculation.

In summary, we believe we have quantitatively explained the major features of the temperature and frequency dependence of the proton spin relaxation in the linear-chain compound TMMC. The theory is algebraically simple and physically it is readily interpreted in some detail. Increased understanding will come with experiments on other nuclei, notably  $^{15}\text{N}$ , and with the application of more sophisticated theories.

#### ACKNOWLEDGMENTS

We would like to thank N. Nighman for growing the TMMC crystal and Dr. M. Mali for doing the high-temperature (90–300 °K) measurements. We also thank Professor V. Jaccarino, Dr. J. P. Boucher, and Professor P. Pincus for useful suggestions. Two of us (C. S. and F. B.) gratefully acknowledge the hospitality of the Physics Department of the University of California, Santa Barbara, during the periods when much of this work was completed.

†Work supported in part by the National Science Foundation under Grant Nos. GP 28917 and GH 36542.

\*Supported in part by Conselho Nacional de Pesquisas, Brazil. Permanent address: Instituto de Fisica, Universidade Federal do Rio Grande do Sul, Porto Alegre, Brazil.

‡Supported in part by a NATO research grant, as a visiting scientist at the University of California, Santa Barbara, Calif., during the period when much of the work reported here was performed.

<sup>1</sup>R. E. Dietz, F. R. Merrit, R. Dingle, D. Hone, B. G. Silbernagel, and P. Richards, *Phys. Rev. Lett.* **26**, 1186 (1971).

<sup>2</sup>F. Borsa and M. Mali, *Phys. Rev. B* **9** (to be published).

<sup>3</sup>P. M. Richards, *Phys. Rev. Lett.* **28**, 1646 (1972).

<sup>4</sup>M. Blume and J. Hubbard, *Phys. Rev. B* **1**, 3815 (1970); J. Hubbard, *J. Phys. Chem.* **4**, 53 (1971).

<sup>5</sup>F. B. McLean and M. Blume, *Phys. Rev. B* **7**, 1149 (1973).

<sup>6</sup>T. Moriya, *Progr. Theor. Phys.* **28**, 371 (1962).

<sup>7</sup>M. E. Fisher, *Am. J. Phys.* **32**, 343 (1964).

<sup>8</sup>The pulsed spectrometer was built by M. R. McHenry and B. G. Silbernagel, following the design by W. G. Clark [*Rev. Sci. Instr.* **35**, 316 (1964)].

<sup>9</sup>B. W. Mangum and D. B. Utton, *Phys. Rev. B* **6**, 2790 (1972).

<sup>10</sup>R. Kubo, in *Fluctuation, Relaxation, and Resonance in Magnetic Systems*, edited by D. Ter Haar (Plenum, New York, 1961).

<sup>11</sup>G. Reiter (unpublished); J. P. Boucher (unpublished).

<sup>12</sup>L. R. Walker, R. E. Dietz, K. Andrea, and S. Darak, *Solid State Commun.* **11**, 593 (1972).

<sup>13</sup>R. Brout and H. Thomas, *Physics* **3**, 317 (1967).

<sup>14</sup>J. E. Gulley, D. Hone, V. Jaccarino, and C. Scherer, *Rev. Bras. Fis.* (to be published).

<sup>15</sup>H. Mori and K. Kawasaki, *Progr. Theor. Phys.* **27**, 529 (1962).

<sup>16</sup>See H. Tomita and H. Mashiyama, *Progr. Theor. Phys.* **28**, 1133 (1972).

<sup>17</sup>J. E. Gulley, D. Hone, D. J. Scalapino, and B. G. Silbernagel, *Phys. Rev. B* **1**, 1020 (1970).

<sup>18</sup>The dependence on  $\Gamma^{-1}$  ( $Q=0$ ) is more general than the particular temperature dependence resulting from the present approximation for  $\Gamma_q$  using  $M_2$  and  $M_4$  {see Ref. 3, where this  $T^{3/2}$  behavior of  $\Gamma(Q=0)$  was obtained from the moments calculated by S. Lovesey and R. Meserve [*Phys. Rev. Lett.* **28**, 614 (1972)]}. The inclusion of  $M_6$  (Ref. 16) or application of the theory of McLean and Blume (Ref. 5) suggests  $\Gamma(Q=0) \sim T$ , whereas experiment seems closer to  $T_1 \sim T^2$ .

<sup>19</sup>M. T. Hutchings, G. Shirane, R. J. Birgeneau, and S. L. Holt, *Phys. Rev. B* **5**, 1999 (1972).

<sup>20</sup>B. Morosin and E. J. Graeber, *Acta Cryst.* **23**, 766 (1967).

<sup>21</sup>M. Suzuki, *Phys. Lett.* **35A**, 23 (1971); *Progr. Theor. Phys.* **46**, 1054 (1972).

<sup>22</sup>L. L. Liu and H. E. Stanley, *Phys. Rev. Lett.* **29**, 927 (1972).